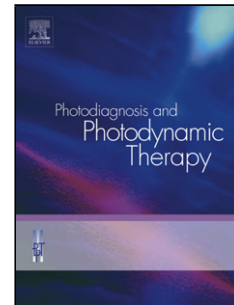


Accepted Manuscript

Title: Development of a handheld fluorescence imaging device to investigate the characteristics of protoporphyrin IX fluorescence in healthy and diseased skin

Author: Olena Kulyk Sally Ibbotson Harry Moseley Ronan Valentine Ifor Samuel



PII: S1572-1000(15)30033-8
DOI: <http://dx.doi.org/doi:10.1016/j.pdpdt.2015.10.002>
Reference: PDPDT 701

To appear in: *Photodiagnosis and Photodynamic Therapy*

Received date: 10-6-2015
Revised date: 10-9-2015
Accepted date: 6-10-2015

Please cite this article as: Kulyk Olena, Ibbotson Sally, Moseley Harry, Valentine Ronan, Samuel Ifor. Development of a handheld fluorescence imaging device to investigate the characteristics of protoporphyrin IX fluorescence in healthy and diseased skin. *Photodiagnosis and Photodynamic Therapy* <http://dx.doi.org/10.1016/j.pdpdt.2015.10.002>

This is a PDF file of an unedited manuscript that has been accepted for publication. As a service to our customers we are providing this early version of the manuscript. The manuscript will undergo copyediting, typesetting, and review of the resulting proof before it is published in its final form. Please note that during the production process errors may be discovered which could affect the content, and all legal disclaimers that apply to the journal pertain.

Development of a handheld fluorescence imaging device to investigate the characteristics of protoporphyrin IX fluorescence in healthy and diseased skin

Olena Kulyk^a, Sally Ibbotson^{b,c*} s.h.ibbotson@dundee.ac.uk, Harry Moseley^{b,c}, Ronan Valentine^{b,c}, Ifor Samuel^{a*} idws@st-andrews.ac.uk

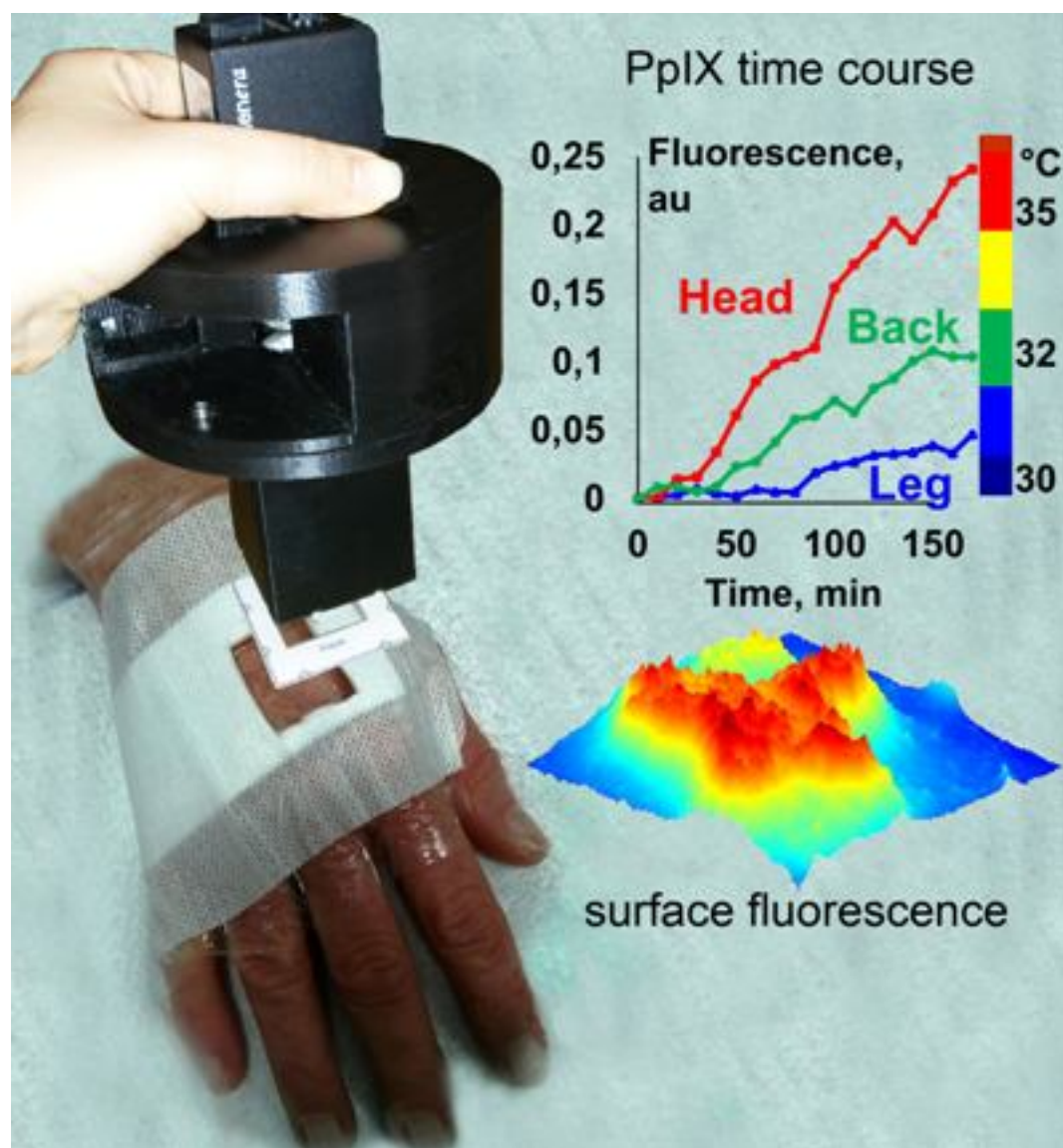
^aOrganic Semiconductor Centre, SUPA, School of Physics and Astronomy, The University of St Andrews, North Haugh, St Andrews, Fife KY16 9SS, UK

^bThe Photobiology Unit, University of Dundee, Ninewells Hospital & Medical School, Dundee, UK

^cThe Scottish Photodynamic Therapy Centre, Ninewells Hospital & Medical School, Dundee, UK

*Corresponding authors.

Graphical Abstract



Highlights

We developed a handheld device and a time course method for fluorescence imaging

The device can be used to study PpIX formation in healthy and diseased skin

PpIX fluorescence grows throughout the 3 hours prior to treatment

The fluorescence intensity varies between diagnoses and individuals

The fluorescence depends on the body site, possibly due to differences in temperature

Abstract

Background

Topical Photodynamic therapy (PDT) is an effective treatment for superficial non-melanoma skin cancers (NMSC) and dysplasia. During PDT light activates the photosensitiser (PpIX), metabolised from a topical pro-drug. A combination of PpIX, light and molecular oxygen results in inflammation and cell death. However, the outcomes of the treatment could be better. Insufficient biosynthesis of PpIX may be one of the causes of incomplete response or recurrence. Measuring surface fluorescence is usually employed as a means of studying PpIX formation. The aim of this work was to develop a device and a method for convenient fluorescence imaging in clinical settings to gather information on PpIX metabolism in healthy skin and NMSC with a view to improving PDT regimes.

Methods

A handheld fluorescence camera and a time course imaging method was developed and used in healthy volunteers and patients diagnosed with basal cell carcinoma (BCC) and actinic keratosis (AK). The photosensitiser (precursor) creams used were 5-aminolaevulinic acid (ALA; Ameluz[®]) and methyl aminolevulinate (MAL; Metvix[®]). Pain was assessed using a visual analogue score immediately after the PDT.

Results

Fluorescence due to PpIX increases over three hours incubation in healthy skin and in lesional BCC and AK. Distribution of PpIX fluorescence varies between the lesion types and between subjects. There was no significant correlation between PpIX fluorescence characteristics and pro-drug, diagnosis or pain experienced. However, there was a clear dependence on body site

Conclusion

The device and the method developed can be used to assess the characteristics of PpIX fluorescence, quantitative analysis and time course. Our findings show that body site influences PpIX fluorescence which we suggest may be due to the difference in skin temperature at different body sites.

Keywords: PDT; Fluorescence; Protoporphyrin IX; Time course imaging; Handheld camera.

Introduction

Topical Photodynamic therapy (PDT) has been widely used in dermatology for the treatment of superficial non-melanoma skin cancer (SNMSC) and dysplasia with overall 70-90% clearance rates^{1,2,3}. There are British and International Guidelines for the use of PDT in these conditions^{1,2}. The most common diagnoses treated by PDT are superficial basal cell carcinoma (sBCC), Bowen's disease (BD), and actinic keratosis (AK)^{1,2,3}. AK is a pre-malignant skin condition arising as a consequence of chronic sun exposure and if left untreated can progress to squamous cell carcinoma (SCC)⁴. Bowen's disease is carcinoma in situ and can again progress to invasive SCC. It commonly occurs on the lower legs. BCC is the commonest skin cancer and superficial lesions are often low risk but multiple. PDT is an effective treatment modality for large, multiple, superficial, low risk tumours, field carcinogenesis or dysplasia, as well as in cases when repeated treatments are needed³ such as immunosuppressed patients, including organ transplant recipients⁵. AK and sBCC respond better to PDT than nodular BCC, arguably due to the fact that the pro-drug used is taken up and metabolised more efficiently in the superficial layers of skin than in deeper layers⁶. PDT results in excellent cosmetic outcomes, and healing^{1,2}. However, results could be improved and based on our Scottish experience, 26% of the lesions require more than one cycle of treatment³. During treatment the pro-drug is applied topically (5-aminolaevulinic acid (ALA), Ameluz[®] or methyl aminolevulinate (MAL), Metvix[®]) to the lesion. The pro-drug is taken up and it metabolises to photosensitiser (PpIX) selectively in abnormal cells, reaching higher concentrations in lesions⁷. Light (centred at 630 nm, 75 J/cm² in our practice, although 37-150 J/cm² may be used) is applied to excite PpIX from the ground state. The absorption of light leads to a singlet state that can undergo intersystem crossing to a long-lived triplet state which can in turn excite molecular oxygen leading to the generation of singlet oxygen and other reactive oxygen species (ROS) that induce oxidative stress and cell death⁸. Alternatively the singlet state of PpIX can decay back to the ground state resulting in fluorescence⁸. Fluorescence is therefore an indicator of the concentration of PpIX in tissue and can be used in PDT diagnostics and clinical research^{8,9}. The efficacy of PDT depends on the combination of the three key treatment parameters: PpIX distribution, molecular oxygen and light delivery¹⁰.

Thus, although PDT is widely and extensively used the response to the treatment could be improved. One of the causes of incomplete response or recurrence to PDT may be insufficient accumulation of PpIX throughout the diseased tissue^{11,12,13}. An optimal concentration of PpIX after application of ALA as pro-drug has been reported to be at six hours and with the full incubation period being 24 hours in that study¹⁴. PpIX

concentration increases and reaches a plateau in both BCC and AK lesions after 13 hours of continuous application of MAL cream¹⁵. However, the recommended time to start the treatment is 3 hours^{1,2}. Yet, there is a limited information about PpIX metabolism at shorter periods of time^{14,15, 16}. Our work aims to develop improved instrumentation for detecting PpIX and apply it to filling these gaps in the knowledge about PpIX building-up during the first three hours from the application of the topical pro-drug. This information could potentially be used to optimise treatment parameters. In addition, we aimed to establish if there were any distinct fluorescence patterns for healthy skin, AK and BCC lesions, or differences between the pro-drugs.

There are various methods of estimating PpIX accumulation in skin. One of the simplest ways is to use Wood's lamp for visual assessment and grading of surface fluorescence of PpIX before PDT. Our unit has previously used an optical biopsy system (OBS) consisting of a 405 nm diode laser and fibre-coupled spectrometer to give measurements of the fluorescence spectrum of PpIX at one point on the skin. This system was used to study the photobleaching of PpIX fluorescence decay during treatment and reverse Monte Carlo modelling was used to learn about the PpIX distribution in skin^{17,18,19}. Other groups have developed optical probes for quantitative measurement of real PpIX concentration and used it for studying the biosynthesis of PpIX from ALA precursor¹⁶. Another technique is fluorescence microscopy for histological assessment of PpIX distribution⁶. There have been reports of custom built optical spectrometers for medical applications^{9,11,13,20,21,22,23,24,25}. However, most of the systems are bulky and have not been designed for time course imaging and analysis.

There were a few recent reports on smaller imaging systems for time course measurements [22,23,24,25,]. . In [22] an imaging platform based on a smartphone has similar conceptual optical design: there was an excitation source build as an array of LED placed around the camera with an emission filter on top of the camera. This device was able to image physiologically relevant concentration of PpIX in liquid TiO₂ scattering in-house made PpIX phantoms in a cuvette. The device was designed for bringing PDT in developing countries to reduce the cost of PDT lamps and proven to be suitable for delivering PDT dose of red light; the imaging was an additional modality for detecting PpIX fluorescence. In [23] an imaging platform based on a smartphone has some similarities of optical design: there was an excitation source consisting of an array of LED placed around the camera with an emission filter on top of the camera. This device was able to image physiologically relevant concentrations of PpIX in liquid phantoms using TiO₂ nanoparticles to give scattering. The device was designed for bringing PDT to developing countries to

reduce the cost of PDT lamps and proved to be suitable for delivering PDT dose of red light; the imaging was an additional modality for detecting PpIX fluorescence. In [24 and 25] the authors use portable handheld device which combines PDT treatment and imaging modalities. The imaging system is based on an array of 400 nm peak wavelength LED for excitation with 50 mW/cm² optical output and 475 nm long pass filter. A Sony DSC-H50 colour digital was used for the imaging. Custom software written in Matlab was used to analyse red and green pixel values for PpIX fluorescence and auto-fluorescence correspondingly. In [24] 54 lesions (21 BCCs, 22 AK, and 11 seborrheic keratosis SK) were used in the study to establish if auto-fluorescence combined with PpIX assisted fluorescence can be used for optical detection of NMSC. ALA solution was applied to the lesions and the fluorescence was imaged at 15, 30, 45 and 60 minutes in a dark room. They found noticeable differences between the autofluorescence in healthy and diseased skin; PpIX fluorescence increased the contrast at the lesion margins. In the following study [25] 8 BCC lesions on different anatomical sides were studied using MAL as PpIX precursor. PpIX fluorescence was imaged 3 hours after application of MAL i.e. just before PDT treatment and in addition immediately treatment. These measurements were made for both the first and the second PDT treatment, which were performed one week apart. They found that the fluorescence was different for lesions at different anatomical sites; it was higher on the lip of one subject compared to the eye lid of another subject. The fluorescence was higher before the second PDT session. This system is one of the best available systems for repeated measurements of PpIX and autofluorescence. In comparison to this system, our system has lower excitation irradiance, 0.1 mW/cm² and the illumination is synchronised with the image acquisition. The synchronisation brings several benefits. It helps to reject ambient light and improves signal to noise. This in turn enables the use of low intensities (eliminating any possibility of photobleaching) and faster measurements.. In addition we developed a specific alignment procedure and camera displacement compensation image analysis to take into account operator tolerance and analyse identical area in all time course images with accurate referencing to the skin and the lesions. The clinical focus of our study was exploring the first three hours of PpIX metabolism in healthy skin and lesions to guide potential improvements in the treatment protocols.

Here we report the development of a hand-held fluorescence imaging camera and its application for the study of PpIX fluorescence characteristics of both healthy and diseased skin. Our portable fluorescence imaging camera measures the spatial distribution of surface PpIX fluorescence and allow for convenient quantitative clinical measurements. The excitation for the camera has the same wavelength as the OBS

system, 405 nm, but allows for studying fluorescence from large areas instead of a point. Fluorescence is detected at 635 ± 5 nm which is the peak of the emission of PpIX. The camera allows fast acquisition of normal images and fluorescence images. It can access any site on the body, has fixed focal distance, shielded from direct ambient light, and allows precise alignment at and referencing to the study area during the time course measurements. We have used the camera in a small study on healthy volunteers and patients with AK and BCC lesions using topical ALA (Ameluz™) and methyl aminolevulinic acid (Metvix). Here we report on the results on PpIX accumulation during three hours of incubation from the application of the pro-drugs and discuss the limitations and clinical relevance of PpIX fluorescence diagnostics. We introduce a few improvements to fluorescence imaging and analysis such as easy access to the patient, the possibility of carrying out the experiment with dimmed lights, accurate referencing of the fluorescence images to the lesion, and an image processing procedure to compensate for displacement of the camera. This work is a first clinical attempt to use fluorescence imaging for studying PpIX formation in NMSC in a time course. Finally we discuss whether there is a correlation between fluorescence and pain, the type of photosensitizer pro-drug and the diagnosis and speculate on the effect of temperature at different body sites.

Methods

Fluorescence imaging system

Fluorescence was imaged using a custom built camera which was developed at the University of St Andrews and built as a prototype device. As the device is not CE marked, it was examined for electrical safety, optical output, allergic reactions and infection control and approved for the research at the Photobiology Unit, Ninewells hospital by the Instrumentation Department at Ninewells hospital and Medical School. The device consists of a Lumenera LM075M CCD camera which connects to and is powered from a laptop via a USB 2.0 interface. An optical lens with a tuneable focal length and an aperture is mounted to the camera; the focus is set to 8.5 cm and checked before each experiment. Once it is set it does not change during the experiment. After a normal image of the skin was acquired under 405 nm illumination, a threaded Thorlab interference band pass filter, FL635 with central wavelength (CWL) of 635 ± 2 nm and full width at half maximum (FWHM) of 10 ± 2 nm was attached to the top of the lens to detect only the peak of the PpIX emission spectrum.

The illuminator for the camera, which serves as an excitation source for PpIX and illumination for monochromatic images of the skin, is a ring of 16 low power 405 nm LEDs mounted on a custom made round shaped printed circuit board (PCB) with an opening in the middle for the lens. The illuminator is powered from a 9 V battery connected to a MOSFET switch and controlled by a USB 2.0 development module FTDI UM245R which turns the switch on and off. The illuminator is connected to a laptop via a USB 2.0 cable. The illumination and the camera are controlled via a simple graphical user interface written in Matlab. The exposure time for normal images is 0.1 ms, fluorescence images are taken with 16.0 ms exposure. The illumination is pulsed when an image is acquired; the duration of the pulse depends on the acquisition time. The optical output power was measured at a distance of 8.5 cm and was found to be 0.1 mW/cm². UV, UVA and blue light exposure limits allow using the device without any special precautions as long as the device is not placed directly on the unprotected eye. The camera does not become hot and is electrically and optically safe.

A custom casing was designed to contain the illuminator, the battery, and the camera; it has a shielded rectangular tube which provides fixed focal distance to the skin site and easy alignment to the study area. The casing was designed in Rhino 3D CAD software and printed with a RoboSavvy MakerBot® Replicator® desktop 3D printer using MakerBot® polylactide (PLA) bio-thermoplastic filament. The material for the casing is inert and is used as a stand-off, not in contact with the skin – the device is placed on a disposable reference frame made of laminated paper; this should eliminate the possibility of causing any allergic reactions. The casing has been designed to minimise infection traps, is “wipe clean” and a decontamination protocol has been provided in the standard operation procedure (SOP). The illuminator and camera assembly is shown on the right of figure 1.

The casing was designed to exclude most ambient light so that experiments could be conducted with dimmed lights on. There are alignment marks at the end of the casing's tube which correspond to the alignment marks of the reference frame so that the same area can be measured each time during a time-course experiment. The marking for the reference frame is printed on a standard white office paper, a fluorescence contour is then drawn using an orange fluorescent marker pen, and the frame was laminated. The frame does not dissolve in any solvents used in the creams, or skin secretions. Once fixed to the skin with a tape, it provides a stable reference for repeated imaging of the study site. The whole set up including computer and accessories fits on top of a small hospital trolley (Fig. 1).

Validation of the system using tissue-simulating phantoms, standard fluorescent solutions and in-vivo

The camera was tested by imaging Coproporphyrin standard solution, in house made PpIX solid fluorescence phantoms, and PpIX fluorescence from healthy skin. The results were compared with spectral measurements taken with the optical biopsy system (OBS). The base for the phantoms was room temperature vulcanised silicone polymer which has similar refractive index to skin. Alumina powder was added to mimicking the scattering properties of the skin²⁶ and PpIX added to give fluorescence. Two parts, A and B of RHODORSIL RTV 141 polymer were mixed in a 1:10 ratio, 4% of alumina scattering powder was added to the mixture, and Protoporphyrin IX P8293 - ≥95% from SIGMA-ALDRICH were dissolved in Methanol. A range of PpIX concentrations of 10, 20, 40, 80, 160, 320 and 640 nM in the phantoms was made for the test. PpIX solution was thoroughly mixed with the silicone polymer and alumina powder and left at room temperature to vulcanise. The phantoms normally vulcanise and the methanol evaporates after 72 hours. We found our camera could successfully image PpIX fluorescence from all the test samples, and then proceeded to image fluorescence from NMSC of two patients, P1 with a BCC lesion and P2 with one AK and two BCC lesions in order to select the appropriate settings for the device.

Pilot clinical trials – study design

A clinical study was conducted to determine the applicability of this device for fluorescence imaging diagnostics, to gather fluorescence images in normal skin and in diseased tissue from different lesions and to fill gaps in knowledge about PpIX fluorescence and time course using two types of pro-drugs and two types of lesions – Ameluz[®] and Metvix[®] administered for BCC and AK. The study was approved by the University of St Andrews Teaching and Research Ethics Committee (UTREC) Ref.: PA10783. The study was conducted in compliance with good clinical practice (GCP) laid down in The Medicines for Human Use (Clinical Trials) regulations 2006 No. 1928. There was no requirement for clinical trial authorisation (CTA) from the UK Medicines and Healthcare products Regulatory Agency (MHRA) as the imaging device was assessed by Professor George Corner, NHS Tayside Head of Instrumentation, as being a prototype and was fit for use in this study alone. The study was also approved by the East of Scotland Research Ethics Service (EoSRES) Committee (REC Ref # 13/ES/0151). Study subjects were identified and recruited from the Photobiology Unit healthy volunteer panel and patient referrals to the Photobiology Unit for photodynamic therapy. Written informed consent was obtained from all subjects before any study-specific activity commenced.

The inclusion criteria for the healthy volunteers were the following: age 18 years and over (age matched to patient cohort as far as practicably possible), both males and females, capable of giving informed consent and able to understand and adhere to the protocol's requirements and having no evidence of active skin disease. The exclusion criteria were the following: anyone with known allergy to Metvix or Ameluz or known to have a light sensitivity disorder. The inclusion criteria for the patients were the following: patients presenting with superficial non-melanoma skin cancer (BCC) and dysplasia (AK) of 18 years age and over, both males and females, capable of giving informed consent and able to understand and adhere to the protocol's requirements. The exclusion criteria for the patients were: patient's skin lesion had had previous treatment within the last four months, patients who were unable to give informed consent, patients with known allergy to Metvix or Ameluz or known to have a light sensitivity disorder. The information sheets were given at least a day before the study and informed consent was taken on the day of the study.

The study included 10 healthy volunteers: in five Metvix was used as pro-drug and the other five received Ameluz gel topically. The skin at the study area was cleaned with ethanol wipes and left to dry before the measurements. From our previous experience we have seen that PpIX metabolism varies at different body sides²⁷. ALA and MAL as PpIX precursors seem to metabolise to give higher concentrations of PpIX on the inner forearm, with lower concentrations on the lower leg. For the healthy volunteers we selected the middle of the back as the site for study as it accumulates PpIX at a medium concentration - in between that of the forearm and lower leg – and so is the best choice for a baseline.

The patient cohort aimed to include 15 patients: five with biopsy confirmed BCC lesions administered Metvix PDT, five AK diagnoses treated with Ameluz PDT, and another five AK diagnoses treated with Metvix PDT. Due to the timescale of the project the study was terminated after 13 patients meaning that we had two fewer patients than planned for AK treated with Metvix PDT. White light images were taken of each subject before the experiments. The lesions were located on different body sites and varied in size. If the size of a lesion was larger than the size of the reference frame, 3.1 cm x 2.4 cm, we selected a small area for the study and the rest of the area was prepared and treated routinely. The whole area was prepared using gentle curettage without a local anaesthetic (Stiefel™ ring curette) to remove all the crusting. The corners for the reference frame were marked with a marker pen; topical pro-drug was applied to the area of the lesion and a 5 mm rim of normal tissue. Tegaderm™ film and Mepore™ occlusive dressing was prepared to cover the lesion, but leaving the study area open (Fig. 2). The reference frame which has

alignment marks corresponding to the alignment marks at the tube of the camera system, and a bright fluorescent contour, which will appear as a saturated white line on fluorescence images for processing the images, was fixed on top of the occlusive dressing with a tape.

A normal monochromatic image of the lesion was taken, then a band pass filter was inserted and background fluorescence was imaged. The cream was then applied with a wooden spatula, a Tegaderm™ occlusive small dressing was placed on top of the reference frame (Fig. 2 c). The small dressing could be easily lifted up and put back again between the readings. Fluorescence was imaged every 10 minutes. Because Metvix cream is opaque, for each measurement we removed the cream and then re-applied it. For consistency we followed the same procedure for Ameluz gel even though it is transparent and does not affect the imaging.

The measurement procedure was the following. There were two timers, one set for nine minutes, the other for one minute. One minute was allocated to take the dressing off, wipe the cream, take a fluorescence image, and put the cream and the dressing back on. When nine minutes had passed we started the one minute timer. During this minute the small dressing was lifted up, the cream was scraped off with a wooden spatula, the remaining cream was wiped off with a cotton wipe, a fluorescence image was taken; the topical pro-drug from the spatula was applied back on (when this was used up, a small amount of fresh cream or gel was added to keep the area covered all the time) and the small dressing was put back on. After the one minute timer had elapsed, the nine minute timer was started again. The measurements were repeated 18 times during three hours. After three hours the cream was removed, fluorescence was visually assessed and scored using a Wood's lamp as an excitation source and routine PDT was delivered (LED light sources, 630 nm, 75 J/cm²)¹⁷. After the treatment had been completed the patients were given a form to assess their pain level on a visual analogue score (VAS) scale with a score from 0 to 10 corresponding to no pain for 0 points and unbearable 'worst pain imaginable' pain for 10 points.

Image processing and analysis

The reference frame has a highly fluorescent contour – an orange rectangle at the inner edges (Fig. 2c), which is seen as a saturated line in all the fluorescence images. This saturated rectangle helps to select the same area on each image for further analysis. The images were acquired, processed and analysed in MATLAB 2014, Image Acquisition, Image Processing and Computer Vision System Toolbox. The fluorescent alignment rectangle allowed us to compensate for any displacement of the camera between

readings We used the random sample consensus (RANSAC) geometrical transformation to detect matching points on the fluorescent alignment contour between the reference image (normally a background image) and the series of 18 fluorescence images. The fluorescence images were reconstructed - rotated and centred to correspond to the position of the background image. After that the fluorescent contour was cropped out and background fluorescence subtracted. The initial size of the image was 640 x 480 pixels which corresponded to 3.1 mm x 2.4 mm; it was cropped to 540 x 380 pixels leaving 67% of the area for further analysis. This completed pre-processing of the images and prepared them for fluorescence analysis. Various regions of interest (ROIs) were selected and an integrated fluorescence was calculated over the ROIs. The size of the ROIs varied depending on the size of uniform peak fluorescence region. The smallest ROI was 25 x 38 pixels for P004 subject and the largest was 73 x 86 pixels for P013. Fluorescence was correlated to the study area.

Fluorescence homogeneity was calculated in the ROIs and over the whole image at 180 min from the application of the creams. The fluorescence value and pixel indices for local minimum and local maximum for ROI and global minimum and global maximum for the whole image were identified. In order to reduce numerical noise 5 pixel values were averaged at the minima and maxima. The homogeneity was calculated as $1 - \frac{\{global, local\} \max - \{global, local\} \min}{local_mean}$, %.

Statistical data analysis

The statistical significance for the fluorescence time course between healthy volunteers Ameluz and Metvix groups, AK Metvix, AK Ameluz, BCC Metvix, body sites groups (the head & the neck vs lower leg & feet, trunk & hands) groups were estimated by t-test for two-sample assuming unequal variances.

Results

Camera validation tests

Fig. 3 shows emission spectra measured with the OBS system and fluorescence images from the 80 nM PpIX phantom, coproporphyrin solution in HCl, and PpIX fluorescence from a healthy volunteer three hours after application of topical Ameluz gel in an aluminium Finn® chamber for patch tests. We have compared the emission spectra to the fluorescence images taken with the camera. PpIX phantoms have a typical emission peak at 633 nm and a slightly elevated second peak at 700 nm. Coproporphyrin has two peaks at 594 and 653 nm. PpIX fluorescence from the volunteer (after application of Ameluz) has peak at 635 nm

which corresponds to the transmission of the band pass filter. Our camera has high selectivity for 635 nm PpIX emission and rejection of other wavelengths, which is why PpIX fluorescence formed from Ameluz from the healthy volunteer appears brighter on the fluorescent images than the 80 nM PpIX solid phantom or Coproporphyrin solution. Our current procedure does not take account of differences in the optical properties of skin in different individuals; so we are not able to extract real concentrations of PpIX from our measurements. However, all of our subjects have skin types I-III which do not have drastic variation in melanin concentration. This in principle should allow us to compare relative PpIX fluorescence measurements across the individuals.

Preliminary data gathering from BCC and AK lesions

Two patients, subject P1 with a BCC lesion and subject P2 with two BCC and one AK lesion, were imaged prior to finalising the clinical study design in order to select appropriate camera settings. The BCC lesion from subject P1 was imaged three hours after application of Metvix before first and second PDT treatments separated one week apart (Fig. 4). We have observed a reduction in fluorescent area and a drop in fluorescence intensity which shows tumour response to the first PDT treatment and the relevance of using the device for fluorescence diagnostics.

Clinical study

Healthy volunteers: Ameluz and Metvix PpIX fluorescence time course

Our study protocol included 10 healthy volunteers: Metvix® cream was applied to five and Ameluz™ gel to the other five. The Metvix® volunteers group had 6 volunteers instead of the planned 5 as one of the volunteers developed almost undetectable fluorescence. The study site for all of the volunteers was the middle of the back avoiding the paravertebral regions. Fig. 5 shows the fluorescence time course calculated by integrating over the whole area of the images. Background fluorescence was subtracted and the readings normalised to the maximum of the camera. Our findings suggest that there is no obvious difference between Ameluz and Metvix in the resulting fluorescence time courses; Ameluz and Metvix groups are not statistically significantly different, the p-value was found to be 0.3 in two sample t-test with unequal variances. Although there is variation between subjects, concurring with previous findings^{27,28}. PpIX fluorescence was still increasing after three hours incubation.

Fluorescence from eight out of ten volunteers was mostly uniform. Two out of ten volunteers showed slightly spotted patterns which however did not have an obvious correlation to the skin structure.

Patients: Ameluz- and Metvix-induced PpIX fluorescence from BCC and AK lesions at different body sites

The results from 13 patients showed variation in fluorescence patterns between the subjects and between lesions. Some of the lesions with non-hyperkeratotic surfaces and well defined margins had uniform fluorescence over the lesions. Fluorescence started to develop at a smaller area inside visible margins and became visible to the device after about 60 minutes from the application of the pro-drugs (Fig. 6 d). It continued to grow at different rates over different areas on the lesions. For example, in the case of subject P010 an area highlighted with red dashed rectangle (Fig. 6) showed the highest PpIX fluorescence. Such hot spot regions were selected for calculations of an integrated fluorescence time course. In six cases the fluorescence extended beyond the visible borders. However in the other seven cases the fluorescence was evident in only some parts of lesions and in many cases fluorescence developed at areas of the skin that were outside the apparent extent of the lesion, possibly highlighting sub-clinical disease.

On average for 12 patients the fluorescence of the lesion was homogeneous with more than 75 % homogeneity in the ROIs; and for one patient it was heterogeneous with homogeneity equal to 25 %. Over the whole image the fluorescence was heterogeneous with homogeneity less than 21 % on average for 12 patients which indicated the contrast between the peak fluorescence in ROI and the rest of the image including healthy parts of the skin in cases for well-defined fluorescence patterns; the fluorescence was 54 % homogeneous for one patient with poorly defined weak fluorescence.

Fig. 6 b shows an overlap of the fluorescence image on a false colour scale taken after three hours of Metvix application and a monochromatic image of the BCC lesion. There were fluorescent areas outside the visible lesion at the top of the image which did not appear to have evidence of diseased skin to the naked eye. In the case of P005 (Fig. 7) there are two AK lesions similar in size and shape situated on the same foot close to each other. Both of the lesions were treated with Metvix PDT; treatment and study-related measurements were undertaken at the same time for both lesions. One of the lesions, #4, showed much stronger fluorescence over a larger area than the other lesion, #1. Also from the fluorescence image we can see the formation of two halves of the lesion #4 correlating with lesion shape (Fig. 7 a, b). Lesion #1 developed much weaker fluorescence which did not correlate with the shape of the lesion. Interestingly pain score for both of the lesions was the same.

In cases where there was crusting, erosion and/or bleeding after surface preparation the fluorescence signal could be reduced which made fluorescence diagnostics much more challenging (SI 1, SI 2). In such

cases the regions of interest (ROIs) for the integrated fluorescence calculations were selected avoiding these areas.

An integrated fluorescence time course suggested that PpIX fluorescence continued to increase over three hours in all subjects. There was no obvious difference between diagnoses (AK or BCC), nor the pro-drugs (Ameluz or Metvix); p-values for AK Ameluz and AK Metvix group was 0.16, p-values for AK Metvix and BCC Metvix was 0.18. Nor was there a correlation between PpIX fluorescence and pain experienced, the correlation coefficient was -0.18, (SI 4). However, there was an obvious dependence for with body sites. The p-value for the group of the head & the neck vs the lower leg & the feet was 0.0003, and between the group of the head & the neck vs trunk & the hands was 0.001. There was no significant statistical difference between the group of the lower leg & the feet compared to the group of trunk & the hands, p-value was 0.12. Fluorescence was obviously higher at the head and the neck than on the lower leg, the foot, the hand and the back.

Discussion

PpIX fluorescence patterns of AK and BCC lesions and where PpIX fluorescence diagnostics and display of NMSC is useful

It has been reported that PpIX fluorescence does not have absolute correlation to PDT outcomes^{11,12}, yet it has been successfully used to detect early stages of malignant changes in the skin^{29,9,30}. Measurement of fluorescence is the most widely used method employed for non-invasive *in-vivo* imaging of PpIX metabolism, which in turn may be used as a surrogate to optimise PDT parameters.

The fluorescence patterns which we observed so far are consistent with previous reports. In a proportion of the subjects in our study fluorescence developed within visible tumours with definition at tumour margins similar to that reported [20,13]. The cases where fluorescence developed in the areas close to the lesions but without any visible evidence of malignant skin disease is supportive of the pick up of subclinical disease and agrees with the study on wide field PpIX fluorescence imaging for early stage NMSC diagnostics²⁹.

Some of the studies report cases without obvious fluorescence but yet response to PDT^{11,12}. We also saw cases with weak fluorescence. However, our device still was able to detect it and its development over

time. We analysed the time course over hot spot ROIs, and could precisely relate the ROIs on the fluorescence images to the shape of the lesions. Our method does not fully resolve the problem of reduced fluorescence detection in the presence of bleeding, crusting and erosion, which complicates fluorescence diagnostics. Yet, it offers flexibility in selecting ROI and accuracy in correlating it to the lesions which may be useful for some studies.

PpIX fluorescence correlation to the body sites: does skin temperature influence PpIX metabolism at different body sites?

Our results showed higher fluorescence on the head and the neck compared to the lower leg (Fig. 8). This agrees with our previous study on PpIX fluorescence from healthy skin at different body sites which showed lower fluorescence at the lower leg^{27,28}. We speculate that this may be due to the difference in the temperature at different body sites. It is also possible that the higher vascularization of the head and neck compared to the body extremities plays a role. It has been reported that PpIX metabolism is faster at higher temperatures^{31,32}. Skin temperature varies at different body sites and can be displayed with infrared imaging cameras³³ [<http://www.nhrd.nhs.uk/page/92>]. Typical temperatures of the head and the neck have found to be 35-37°C^{34,35}, the lower leg and the “edge” areas of the feet and the hands have lower temperatures of 30-33°C. We estimated typical temperatures of healthy skin at the lesions sites using infrared thermal images reported in the literature (SI 5)^{35,34,36} and correlated this with the fluorescence measurements. The body sites which typically are hotter develop higher fluorescence (Fig. 8) which suggests that the skin temperature may be responsible for the rate of PpIX metabolism; if this hypothesis is true heating up or cooling down would have a significant effect on treatment. There is evidence to show that cooling air to reduce pain has an adverse effect on PDT outcomes³⁷ and increasing the skin temperature results in increased PpIX metabolism^{32,38,39}.

PpIX fluorescence correlation to the pro-drugs used and pain experienced

There is rather conflicting evidence in the literature about pain/fluorescence correlation^{16,13}. Our results suggest that there is no obvious correlation or significant statistical dependence (SI 4). One study [13] reported higher MAL fluorescence compared with ALA. We did not see an obvious difference between ALA or MAL PpIX-induced fluorescence time courses.

Conclusions

A light weight hand-held fluorescence imaging camera that is easy to use in a clinical setting has been introduced and used in a small study of PpIX metabolism. The camera has a 405 nm illumination and PpIX excitation source; a removable band pass filter centered at a 635 nm PpIX emission peak. The camera allows acquisition of monochromatic images of the skin under 405 nm illumination and 635 nm fluorescence images. Custom made bio-plastic casing is shielded from direct ambient light and allows carrying measurements with dimmed lights. Alignment marks on the casing and a corresponding disposable flexible reference frame which is fixed to the skin of a patient with a tape allows imaging and analysing the same area through time course study.

We have designed a fluorescence time course imaging method and analysed results from 11 healthy volunteers and 13 patients. We have not seen an obvious difference in fluorescence time courses between Ameluz and Metvix pro-drugs used (whether in healthy volunteers or in patients) and also did not see a difference between BCC and AK lesions. However, there was dependence of the strength of fluorescence on the body site –fluorescence was lower on the lower leg and higher on the head and the neck. We suggest that this may be caused by lower temperature on the lower leg which may result in slower PpIX metabolism. Our results show that the fluorescence is still increasing three hours after application of the pro-drugs in both patients and healthy volunteers. This suggests that waiting longer after applying the cream could increase PDT response, although loss of specificity at longer incubation periods is a potential concern.

We have seen a large variation in fluorescence between subjects and lesions. There is insubstantial and conflicting current evidence in the literature about pain/fluorescence correlation; our results do not show a correlation.

Although caution is needed in over-interpretation of the results in this small study, it is a first clinical attempt to undertake a time course study using this quantitative fluorescence imaging device. Our findings address some of the gaps in understanding of PpIX metabolism in different lesions at different body sites, using different pro-drugs. We hope that this will lead on to further studies, with a view to optimisation of treatment regimes.

Acknowledgements

The authors are thankful to the research coordinator June Gardner for her help with the regulations, principles and standards of good clinical practice (GCP) of The Medicines for Human Use (Clinical Trials) regulations, guidance with the study protocol, supporting documentation, IRAS application, recruiting and consenting the participants for the study. The authors are also thankful to all of the technical staff: Lynn Fullerton, Andrea Cochrane, Leona Johnston, Laura Patullo, Shelagh Blackwood, Lesley Knight, Ronald Buist, & Gordon Brown at PBU for helping during the measurements on healthy volunteers and patients. OK acknowledges support from the Scottish Funding Council via a SUPA INSPIRE studentship. IDWS was partly supported by EPSRC grant EP/J01771X and a Royal Society Wolfson Research Merit Award. We are grateful to the Alf Stewart Trust for ongoing support of the Scottish PDT Centre.

References

1. L. R. Braathen et al.;¹; “Guidelines on the use of photodynamic therapy for nonmelanoma skin cancer: an international consensus. International Society for Photodynamic Therapy in Dermatology, 2005.,” *J. Am. Acad. Dermatol.* **56**, 125–143 (2007) [doi:10.1016/j.jaad.2006.06.006].
2. C. a. Morton, K. E. McKenna, and L. E. Rhodes;¹; “Guidelines for topical photodynamic therapy: Update,” *Br. J. Dermatol.* **159**, 1245–1266 (2008) [doi:10.1111/j.1365-2133.2008.08882.x].
3. S. H. Ibbotson, R. S. Dawe,¹ and C. a. Morton;¹; “A survey of photodynamic therapy services in dermatology departments across Scotland,” *Clin. Exp. Dermatol.* **38**, 511–516 (2013) [doi:10.1111/ced.12051].
4. C. Quirk et al.;¹; “Progression of Actinic Keratosis to Squamous Cell Carcinoma Revisited: Clinical and Treatment Implications,” *Cutis* **85**(April), 318–324 (2010).
5. A.-M. Wennberg et al.;¹; “Photodynamic Therapy With Methyl Aminolevulinic Acid for Prevention of New Skin Lesions in Transplant Recipients: A Randomized Study,” *Transplantation* **86**(3) (2008).
6. K. Togsverd-Bo et al.;¹; “Protoporphyrin IX formation and photobleaching in different layers of normal human skin: Methyl- and hexylaminolevulinic acid and different light sources,” *Exp. Dermatol.* **21**, 745–750 (2012) [doi:10.1111/j.1600-0625.2012.01557.x].
7. S. H. Ibbotson;¹; “An overview of topical photodynamic therapy in dermatology,” *Photodiagnosis Photodyn. Ther.* **7**(September 2009), 16–23 (2010) [doi:10.1016/j.pdpdt.2009.12.001].
8. E. Buytaert, M. Dewaele, and P. Agostinis;¹; “Molecular effectors of multiple cell death pathways initiated by photodynamic therapy,” *Biochim. Biophys. Acta - Rev. Cancer* **1776**, 86–107 (2007) [doi:10.1016/j.bbcan.2007.07.001].
9. J. Hewett et al.;¹; “Fluorescence detection of superficial skin cancers,” *J. Mod. Opt.* **47**(11), 2021–2027 (2000) [doi:10.1080/095003400417179].
10. F. Hetzel et al.;¹; “Photodynamic Therapy Dosimetry,” *AAPM Report*(88), 30 (2005).

11. M. Fernández-Guarino et al.;¹; , “Six Years of Experience in Photodynamic Therapy for Basal Cell Carcinoma: Results and Fluorescence Diagnosis from 191 Lesions,” *J. Skin Cancer* **2014**, 1–7 (2014) [doi:10.1155/2014/849248].
12. C. Sandberg et al.;¹; , “Photodynamic therapy for ‘difficult-to-treat’ basal cell carcinomas. Do poorly responding BCCs lack accumulation of protoporphyrin IX after ALA/MAL application?,” *Proc. SPIE* **7380**, 73805K – 73805K – 8 (2009) [doi:10.1117/12.822981].
13. C. Sandberg et al.;¹; , “Fluorescence diagnostics of basal cell carcinomas comparing methylaminolaevulinate and aminolaevulinic acid and correlation with visual clinical tumour size,” *Acta Derm. Venereol.* **91**, 398–403 (2011) [doi:10.2340/00015555-1068].
14. C. Fritsch et al.;¹; , “Optimum porphyrin accumulation in epithelial skin tumours and psoriatic lesions after topical application of delta-aminolaevulinic acid.,” *Br. J. Cancer* **79**(9-10), 1603–1608 (1999) [doi:10.1038/sj.bjc.6690255].
15. E. Angell-Petersen et al.;¹; , “Porphyrin formation in actinic keratosis and basal cell carcinoma after topical application of methyl 5-aminolevulinate.,” *J. Invest. Dermatol.* **126**(2), 265–271 (2006) [doi:10.1038/sj.jid.5700048].
16. S. C. Kanick et al.;¹; , “Dual-channel red/blue fluorescence dosimetry with broadband reflectance spectroscopic correction measures protoporphyrin IX production during photodynamic therapy of actinic keratosis,” *J. Biomed. Opt.* **19**, 075002 (2014) [doi:10.1117/1.JBO.19.7.075002].
17. S. H. Ibbotson et al.;¹; , “Photodynamic therapy in dermatology: Dundee clinical and research experience,” in *Photodiagnosis and Photodynamic Therapy* **1**, pp. 211–223 (2004) [doi:10.1016/S1572-1000(04)00045-6].
18. R. M. Valentine et al.;¹; , “Monte Carlo modeling of in vivo protoporphyrin IX fluorescence and singlet oxygen production during photodynamic therapy for patients presenting with superficial basal cell carcinomas.,” *J. Biomed. Opt.* **16**, 048002 (2011) [doi:10.1117/1.3562540].
19. R. M. Valentine et al.;¹; , “Modelling Fluorescence in Clinical Photodynamic Therapy,” *Photochem. Photobiol. Sci.*, 203–213 (2012) [doi:10.1039/c2pp25271f].
20. U. Sunar et al.;¹; , “Quantification of PpIX concentration in basal cell carcinoma and squamous cell carcinoma models using spatial frequency domain imaging.,” *Biomed. Opt. Express* **4**(4), 531–537 (2013) [doi:10.1364/BOE.4.000531].

21. J. Tyrrell, S. Campbell, and A. Curnow,¹; “Validation of a non-invasive fluorescence imaging system to monitor dermatological PDT.,” *Photodiagnosis Photodyn. Ther.* **7**(2), 86–97, Elsevier B.V. (2010) [doi:10.1016/j.pdpdt.2010.03.002].
22. J. Hempstead et al.,¹; , “Low-cost photodynamic therapy devices for global health settings: Characterization of battery-powered LED performance and smartphone imaging in 3D tumor models,” *Sci. Rep.* **5**(May), 10093, Nature Publishing Group (2015) [doi:10.1038/srep10093].
23. R. B. Saager et al.,¹; , “Quantitative fluorescence imaging of protoporphyrin IX through determination of tissue optical properties in the spatial frequency domain,” *J. Biomed. Opt.* **16**(12), 126013 (2011) [doi:10.1117/1.3665440].
24. C. T. Andrade et al.,¹; , “Identification of skin lesions through aminolaevulinic acid-mediated photodynamic detection,” *Photodiagnosis Photodyn. Ther.* **11**(3), 409–415, Elsevier B.V. (2014) [doi:10.1016/j.pdpdt.2014.05.006].
25. K. C. Blanco et al.,¹; , “Fluorescence guided PDT for optimization of the outcome of skin cancer treatment,” *Front. Phys.* **3**(April), 1–7 (2015) [doi:10.3389/fphy.2015.00030].
26. B. W. Pogue and M. S. Patterson,¹; , “Review of tissue simulating phantoms for optical spectroscopy, imaging and dosimetry.,” *J. Biomed. Opt.* **11**(August 2006), 041102–1 – 16 (2015) [doi:10.1117/1.2335429].
27. A. Lesar, J. Ferguson, and H. Moseley,¹; , “An investigation of the fluorescence induced by topical application of 5-aminolaevulinic acid and methyl aminolaevulinate at different body sites on normal human skin,” *Photodiagnosis Photodyn. Ther.* **8**(2), 97–103, Elsevier B.V. (2011) [doi:10.1016/j.pdpdt.2010.12.004].
28. S. H. Ibbotson et al.,¹; , “Characteristics of 5-aminolaevulinic acid-induced protoporphyrin IX fluorescence in human skin in vivo,” *Photodermatol. Photoimmunol. Photomed.* **22**(2), 105–110 (2006) [doi:10.1111/j.1600-0781.2006.00202.x].
29. J. De Leeuw et al.,¹; , “Fluorescence detection and diagnosis of non-Melanoma skin cancer at an early stage,” *Lasers Surg. Med.* **41**(2), 96–103 (2009) [doi:10.1002/lsm.20739].

30. M. Mogensen and G. B. E. Jemec,¹; “Diagnosis of nonmelanoma skin cancer/keratinocyte carcinoma: A review of diagnostic accuracy of nonmelanoma skin cancer diagnostic tests and technologies,” *Dermatologic Surg.* **33**(10), 1158–1174 (2007) [doi:10.1111/j.1524-4725.2007.33251.x].
31. A. Juzeniene et al.,¹; , “Temperature Effect on Accumulation of Protoporphyrin IX After Topical Application of 5-Aminolevulinic Acid and its Methyl ester and Hexylester Derivatives in Normal Mouse Skin,” *Photochem. Photobiol.* **74**(6), 452–456 (2002) [doi:http://dx.doi.org/10.1562/0031-8655(2002)076<0452:TEOAOP>2.0.CO;2].
32. S. Mordon,¹; “A commentary on the role of skin temperature on the effectiveness of ALA-PDT in Dermatology,” *Photodiagnosis Photodyn. Ther.* **11**(3), 416–419, Elsevier B.V. (2014) [doi:10.1016/j.pdpdt.2014.05.004].
33. B. B. Lahiri et al.,¹; “Medical applications of infrared thermography: A review,” *Infrared Phys. Technol.* **55**(4), 221–235, Elsevier B.V. (2012) [doi:10.1016/j.infrared.2012.03.007].
34. J. Živčák et al.,¹; *Methodology, Models and Algorithms in Thermographic Diagnostics*, Springer Heidelberg New York Dordrecht London (2013) [doi:10.1007/978-3-642-38379-3].
35. E. F. J. Ring and K. Ammer,¹; “Infrared thermal imaging in medicine,” *Physiol. Meas.* **33**, R33–R46 (2012) [doi:10.1088/0967-3334/33/3/R33].
36. <http://www.tdmu.edu.ua>,¹; “Medical Thermography / I. Ya. Horbachevsky Ternopil State Medical University, Ukraine,” <http://intranet.tdmu.edu.ua/data/kafedra/internal/klinpat/classes_stud/en/med/lik/ptn/Functional_diagnostics_2_course/2/04_Diagnostics_Methods_pathology_of_internal_organs.htm>.
37. J. Tyrrell, S. M. Campbell, and a. Curnow,¹; “The effect of air cooling pain relief on protoporphyrin IX photobleaching and clinical efficacy during dermatological photodynamic therapy,” *J. Photochem. Photobiol. B Biol.* **103**(1), 1–7, Elsevier B.V. (2011) [doi:10.1016/j.jphotobiol.2010.12.011].
38. P. Juzenas et al.,¹; “Uptake of topically applied 5-aminolevulinic acid and production of protoporphyrin IX in normal mouse skin: dependence on skin temperature.,” *Photochem. Photobiol.* **69**(4), 478–481 (1999) [doi:10.1111/j.1751-1097.1999.tb03315.x].
39. J. T. H. M. van den Akker et al.,¹; “Effect of elevating the skin temperature during topical ALA application on in vitro ALA penetration through mouse skin and in vivo PpIX production in human skin.,” *Photochem. Photobiol. Sci.* **3**(3), 263–267 (2004) [doi:10.1039/b309284d].

Figure Captions

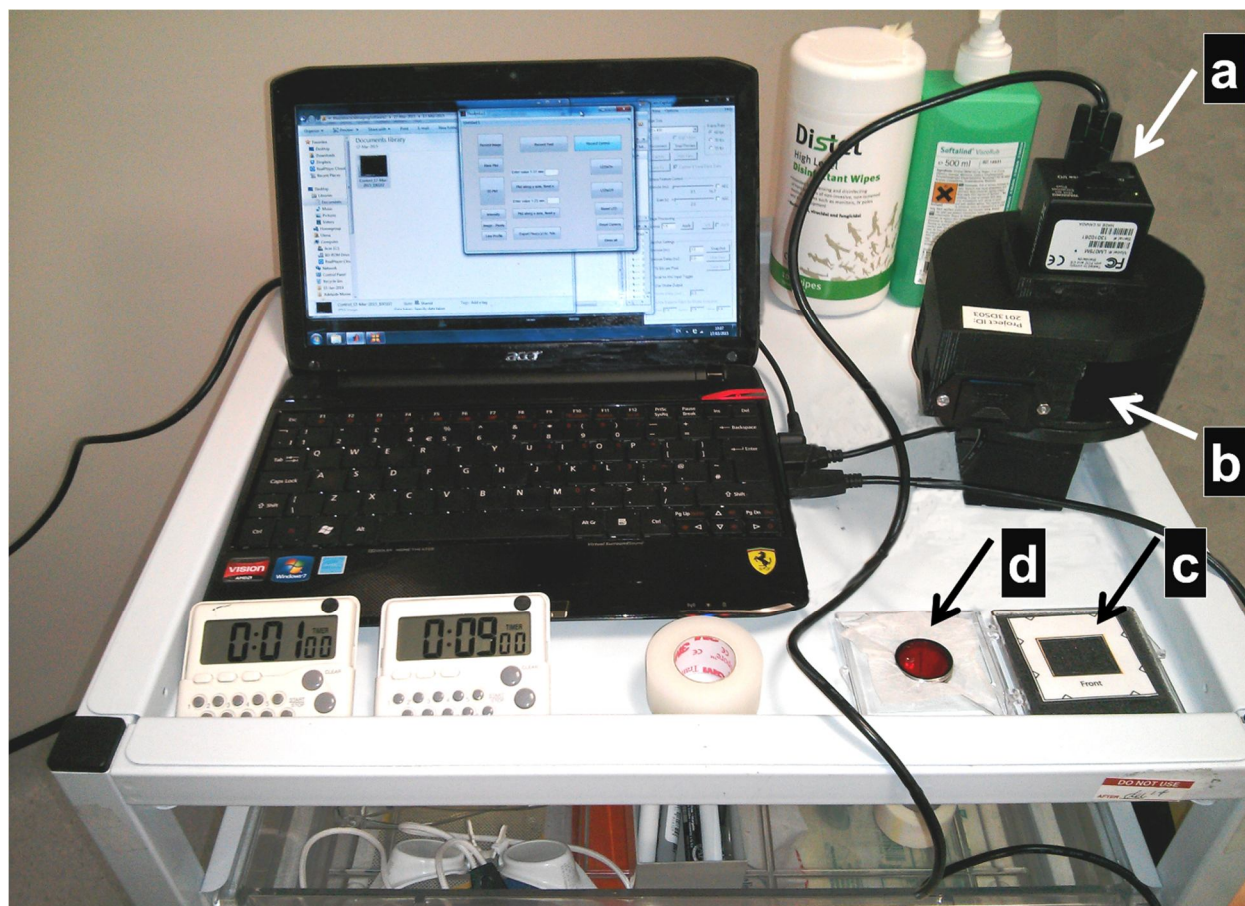


Fig. 1 – The experimental set up on a small hospital trolley (the camera is on the right). a – camera assembly. b – illuminator. c – disposable reference frame. d – emission filter.

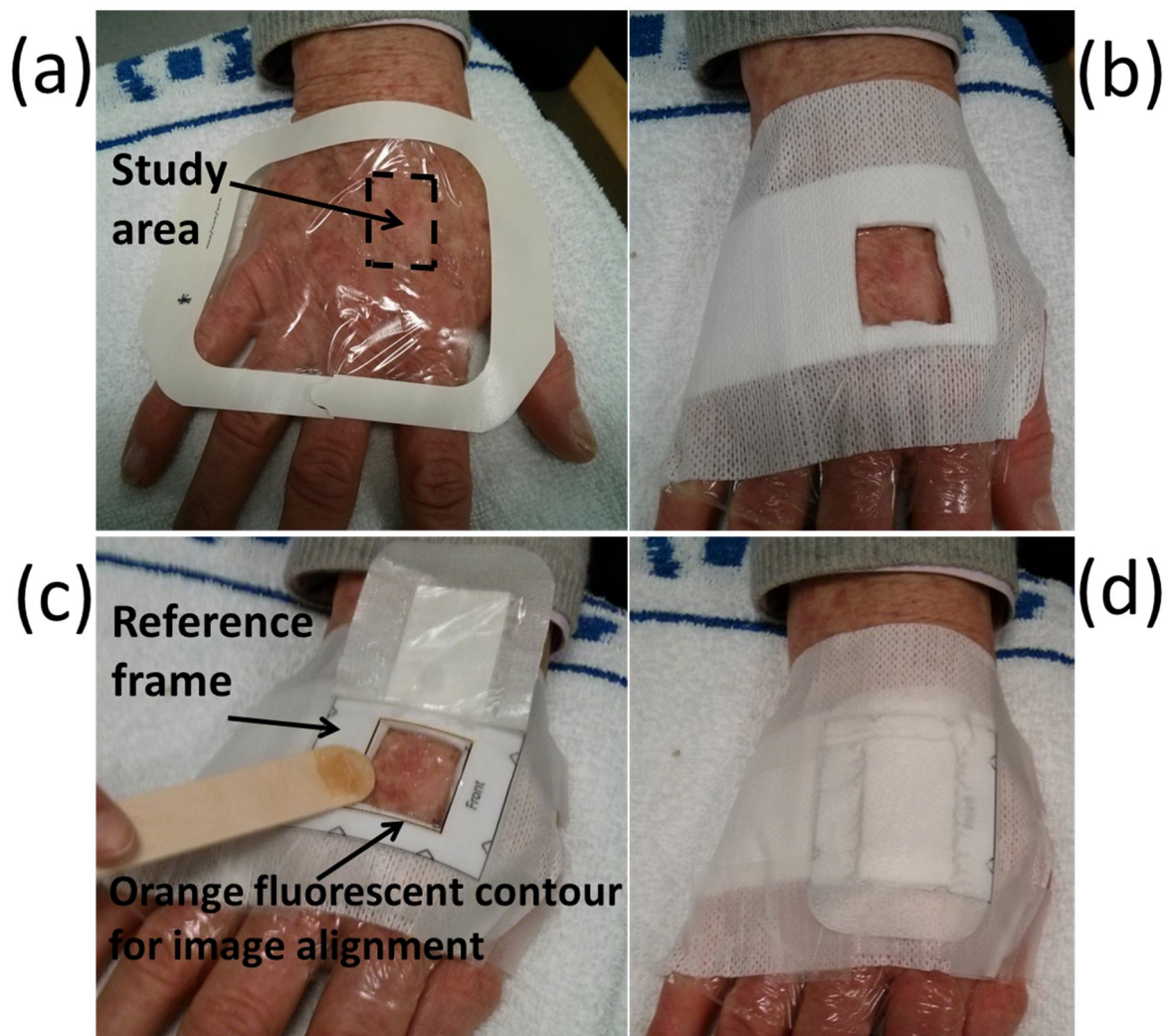


Fig. 2 – Lesion preparation procedure. a – the lesion is prepared with a curette, a small study area is selected, the corners of the area are marked with a marker pen, pro-drug is applied to the lesions outside the study area, transparent Tegaderm™ film is prepared to leave an opening over the study area. b – occlusive dressing is placed on the lesion leaving the study area accessible. c – the reference frame is fixed at the study area with a tape. A small dressing can be lifted up and put back again between the measurements. A wooden spatula is used to remove the cream and put it back after the measurement. d – the area is covered with an occlusive dressing between the measurements.

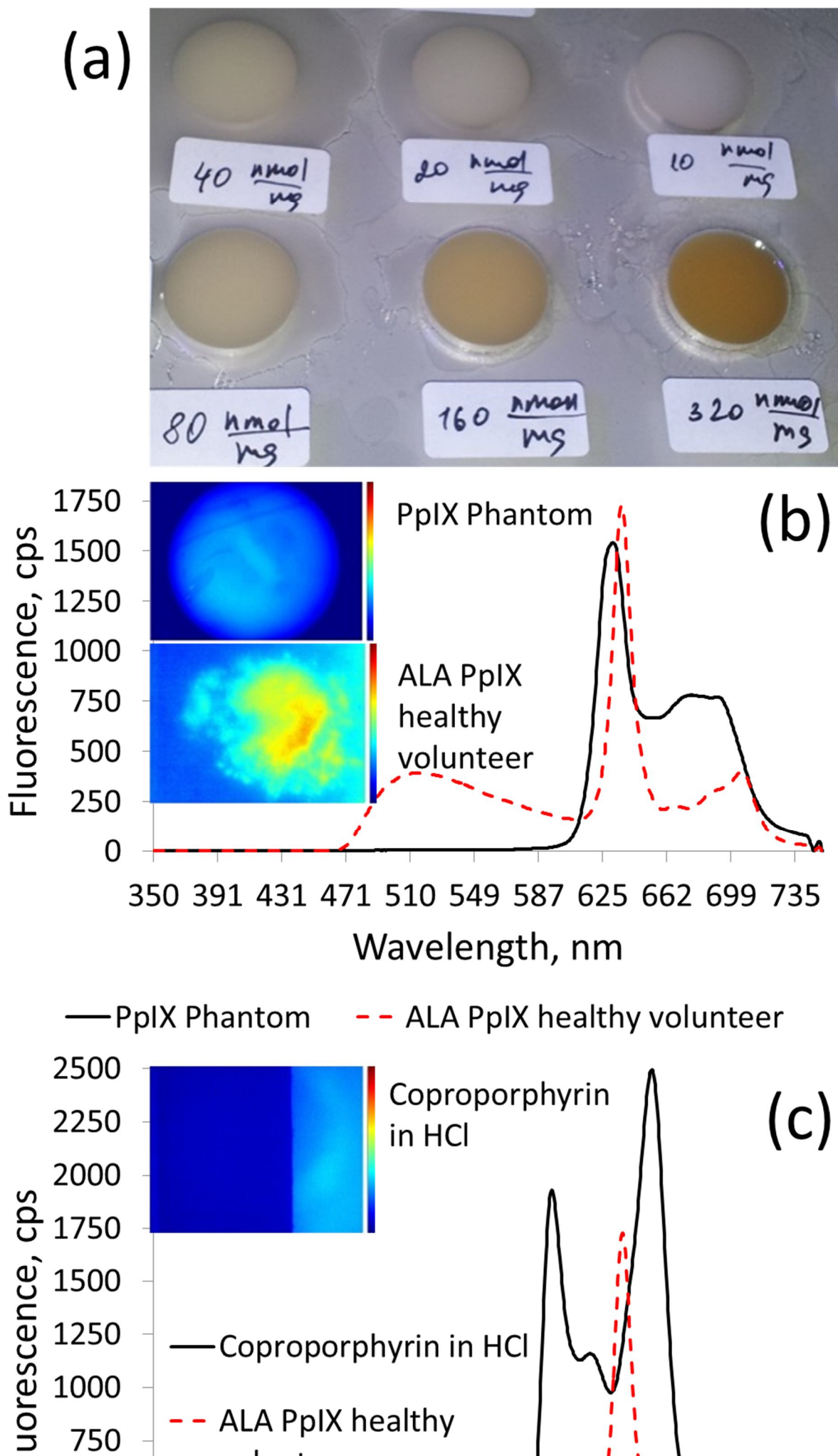


Fig. 3 – Camera validation on PpIX phantoms, Coproporphyrin and Ameluz PpIX fluorescence from the skin of a healthy volunteer. a – a photograph of PpIX solid silicone phantoms with a range of PpIX concentrations. b – OBS measurements of PpIX fluorescence from the phantom with 80 nM concentration and Ameluz PpIX fluorescence from the skin of a volunteer after 3 hours of Ameluz gel application in an aluminium test patch chamber. The image on the top left corner is a fluorescence image of the phantom taken with the camera, the image below is an image of PpIX fluorescence from the volunteer. c – OBS measurements of coproporphyrin fluorescence and Ameluz PpIX fluorescence from the volunteer. The image at the top left corner is a fluorescence image of coproporphyrin solution in a Petri dish. Left half of the Petri dish is covered with a piece of beam blocking paper.

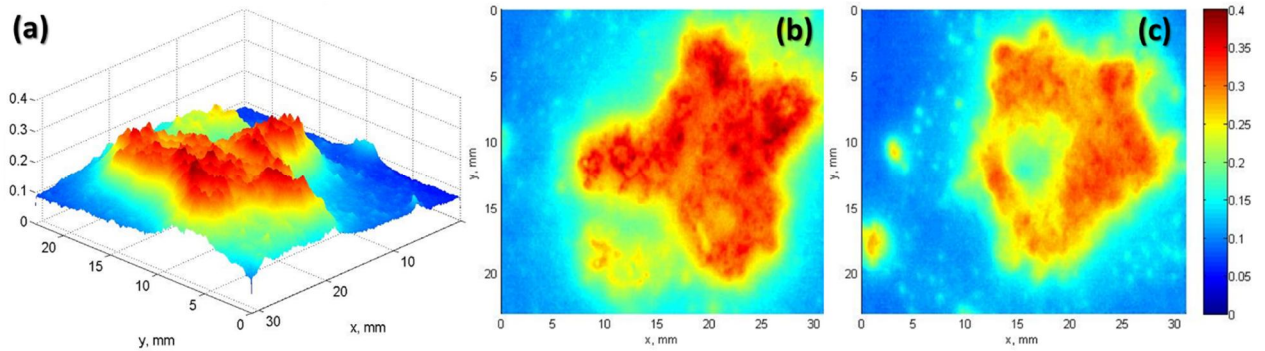


Fig. 4 – The camera validation on PpIX fluorescence from a BCC lesion using Metvix cream. a, b – 3D and 2D surface PpIX fluorescence on a false colour scale taken after 3 hours of Metvix application before the first PDT treatment. c – 2D fluorescence image on the false colour scale before the second treatment (a week later than b). The fluorescence area and the intensity are reduced indicating the response of the lesion to the first PDT treatment.

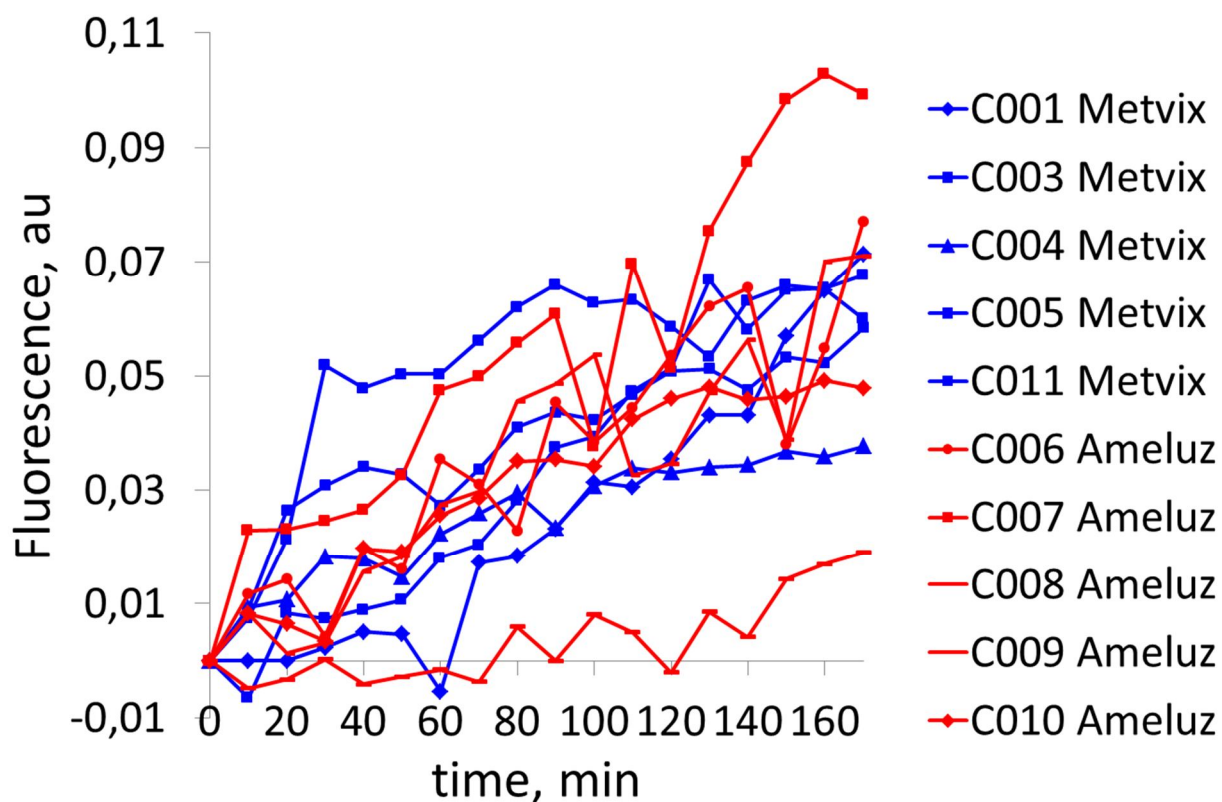


Fig. 5 – Fluorescence time course from healthy volunteers indicating no obvious difference between Ameluz and Metvix metabolism in healthy skin on the middle of the back.

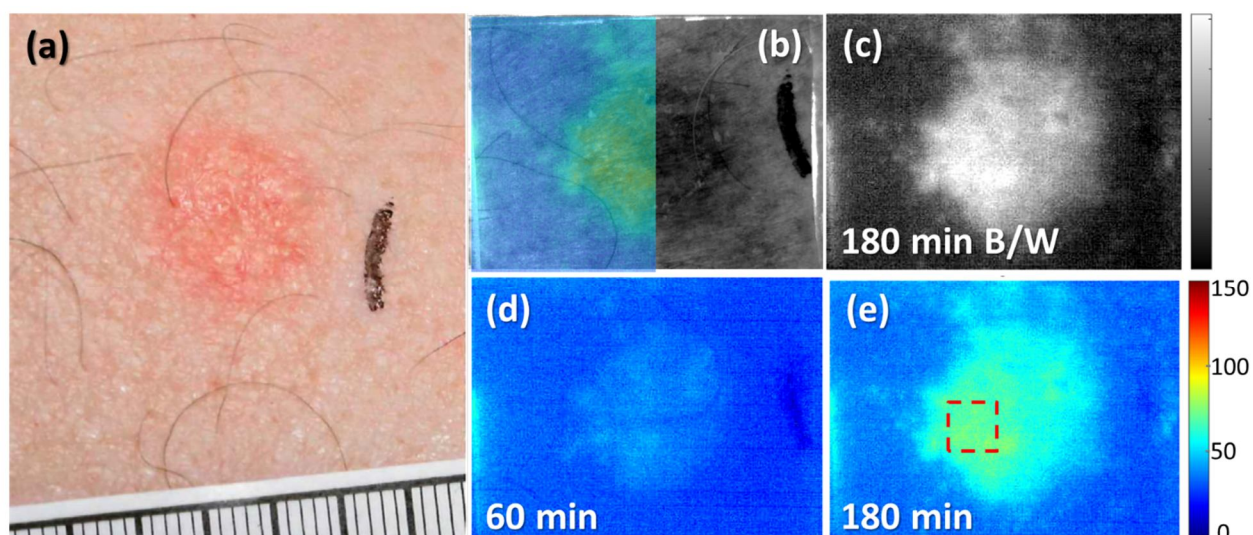


Fig. 6 – P010 – biopsy confirmed BCC lesion administered Metvix PDT: a – a white light image, b – a monochromatic image of the lesion taken with a 405 nm flash. The left half of the image is overlapped with a semi-transparent fluorescence image on the false colour scale taken at 180 minutes after Metvix application which helps to visualise the correlation between the lesion and the fluorescence, c – a monochromatic fluorescence image at 180 min of Metvix application, d – a false colour fluorescence image at 60 min, e – a false colour fluorescence image at 180 min. Red dashed line shows a region of interest which has the highest fluorescence and is used for the calculation of integrated fluorescence in the time course.

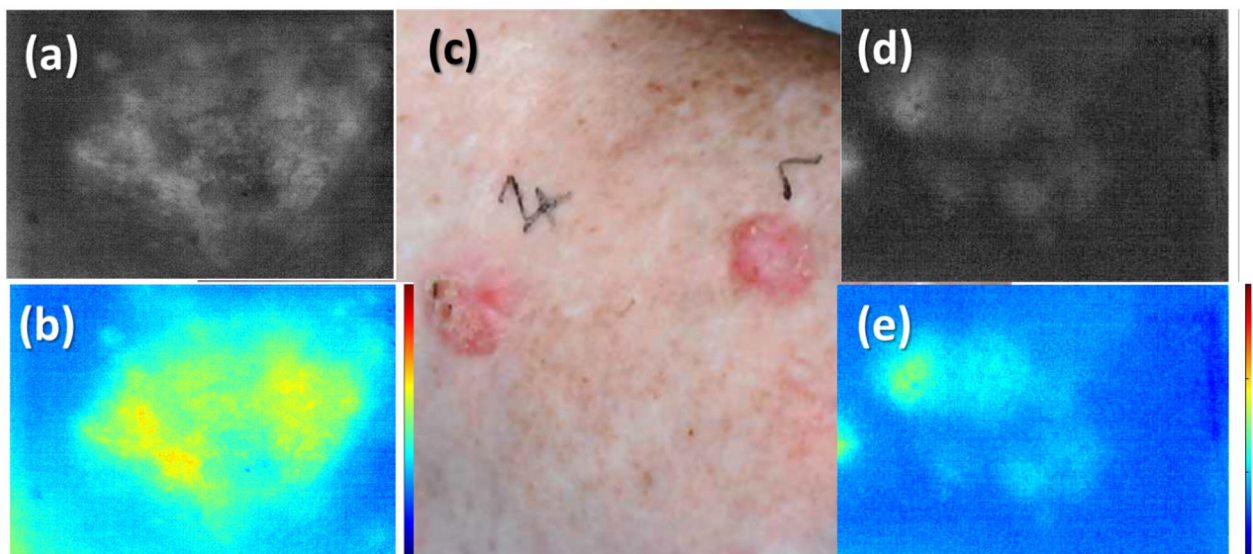


Fig. 7 – P005 - two similar in shape and size AK lesions on the foot treated by Metvix PDT. One lesion is expressing much higher fluorescence than the other a, b – fluorescence images at 180 min on a monochromatic and a false colour scale from #4 lesion. c – a white light image, d, e – fluorescence images at 180 min on a monochromatic and a false colour scale from #1 lesion

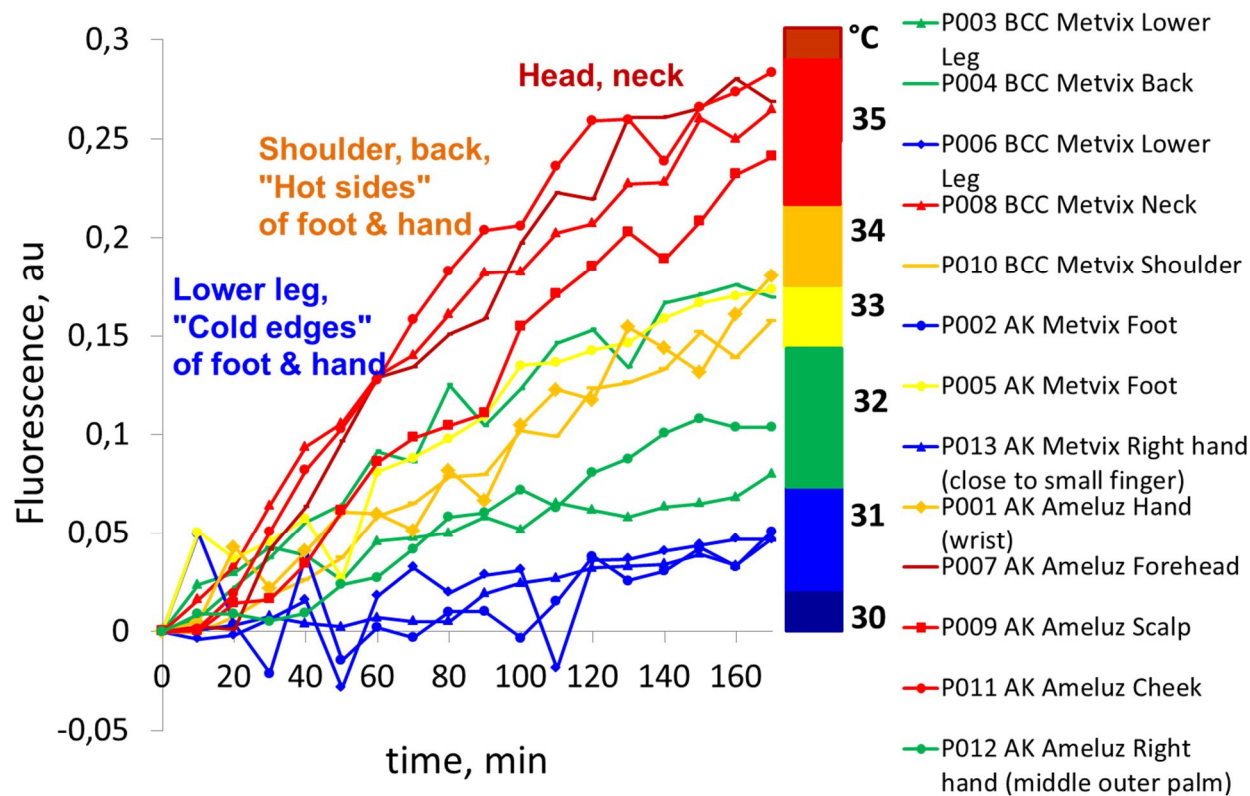


Fig. 8 – Fluorescence time course from 13 patients indicating higher fluorescence on the head and the neck comparing to the lower leg. Temperatures were taken from the literature^{36,34,35}.